Resonance spin flavor precession of solar neutrinos after SNO neutral current data

Bhag C. Chauhan* and João Pulido†

Centro de Física das Interacções Fundamentais (CFIF), Departamento de Física, Instituto Superior Técnico, Av. Rovisco Pais, P-1049-001 Lisboa, Portugal

(Received 20 June 2002; published 23 September 2002)

We present an analysis of the solar neutrino data assuming the deficit of solar neutrinos to originate from the interaction of their transition magnetic moments with the solar magnetic field. We perform fits to the rates only and global fits and consider separately the existing data prior to the announcement of the SNO neutral current results, and the present data. Predictions for the Borexino experiment are also derived. The solar field profiles are taken both in the radiation zone and core of the Sun, and in the convective zone. The latter are chosen so as to exhibit a rapid increase across the bottom of the convective zone and a moderate decrease toward the surface. Regarding the field profiles in the radiative zone and core, it is found that the data show a preference for those cases in which a strong field rests at the solar center with a steep decrease thereafter. For these, the quality of the global fits is as good as the one from the best oscillation solutions and the same as for the convective zone profiles examined. It is also found that the χ^2 of the fits increases when the most recent data are considered, owing to the smaller errors involved. This in turn provides more precise predictions for Borexino than previous ones, thus resulting in a clearer possible distinction between magnetic moment and the currently favored oscillation solutions.

DOI: 10.1103/PhysRevD.66.053006 PACS number(s): 14.60.Pq, 26.65.+t

I. INTRODUCTION

If neutrinos have a sizable magnetic moment [1] their interaction with the solar magnetic field can turn active ν_{eL}'s produced in the core of the Sun into right handed antineutrinos of a different flavor or into sterile neutrinos, unseen in terrestrial experiments. This precession can be resonantly enhanced in matter [2] with the location of the critical density being determined by the neutrino energy, in much the same way as the resonant amplification of oscillations, the Mikheyev-Smirnov-Wolfenstein (MSW) mechanism [3]. For Majorana neutrinos only transition moments are possible and the interaction causes a simultaneous flip of spin and flavor, so that the resulting antineutrino can still be detected in neutrino electron scattering experiments, while in the Dirac case the final state remains undetectable.

The resonance spin flavor precession (RSFP) of solar neutrinos has not received as much attention as oscillations, possibly due to the fact that it requires a large neutrino magnetic moment $O(10^{12}-10^{-11})\mu_B$, far beyond the electroweak standard model value. Nevertheless, several analyses exist [4–8] which show that RSFP provides excellent fits to solar neutrino data, in some cases better than the best oscillation solution, the large mixing angle (LMA) one. While the much expected Kamland results [9] are unavailable and all possibilities remain open, it is very important to test ''nonstandard'' solar neutrino solutions, of which RSFP is the most plausible one. Furthermore, RSFP has the interesting feature of providing a close relationship between the energy shape of the survival probability and the solar magnetic field profile, in the sense that the most suppressed neutrinos have their resonance located in the region where the field is the strongest [10].

In this paper we present an investigation of all the solar neutrino data including the recent SNO results on the charged current day-night effect and the neutral current, based on the assumption that neutrinos undergo RSFP inside the Sun. We neglect the possible contribution of flavor mixing, that is, we take the angle θ_{12} to be too small to play any role in the solar neutrino problem. Only Majorana neutrinos are considered, not only because these have been known for some time to provide better fits to solar data than Dirac ones [4],[1] but mainly because the new SNO neutral current (NC) data seem to exclude the latter if RSFP happens to be the solution.

The available information on the solar magnetic field is still quite limited at present [11] and some authors [12] argue that a large field in the convective zone may not be possible, since it would show up as an 11 year cycle in the SuperKamiokande [13] data, which is known not to be the case. Instead they consider a large field in the lower radiative zone and the core where most neutrinos are produced. It remains unclear, however, whether the sunspot cycle effect extends all the way down to the bottom of the convective zone. Hence, other authors [11,7] favor a profile exhibiting a peak at the bottom of the convective zone with a moderate decrease up to the surface where it nearly vanishes. In our present analyses we consider profiles both in the radiative zone and core, and in the convective zone.

Our main objective is to take a wide class of profiles in the solar interior, extracting from them the RSFP predictions for all neutrino data [13–18] available after the recently an-

*On leave from Govt. Degree College, Karsog (H P) India 171304. Email address: chauhan@cfif.ist.utl.pt

†Email address: pulido@cfif.ist.utl.pt

[1]In fact the early comparisons between Kamiokande and chlorine data alone, with Kamiokande showing a larger signal than chlorine, always favored the possibility that non ν_{eL}'s were active.

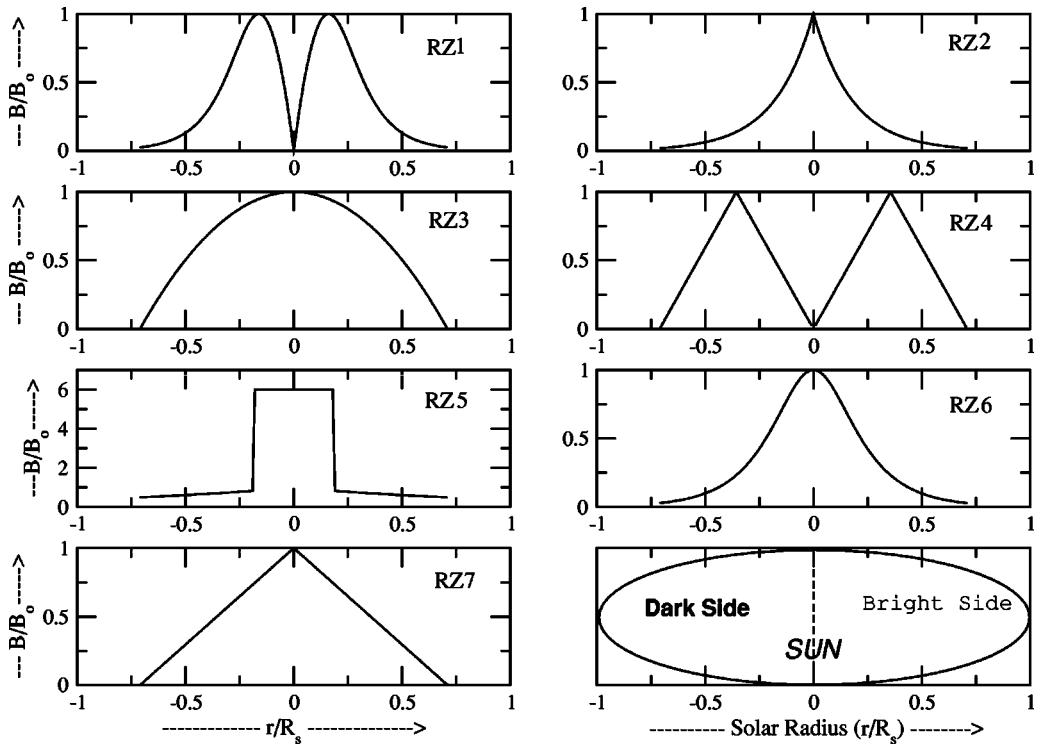

FIG. 1. Solar field profiles in the radiative zone and core. RZ2 and RZ6 are the most favored by the data.

nounced neutral current results from the SNO Collaboration [18] and selecting those profiles which provide the best global fits based on a standard χ^2 analysis. For these we evaluate the 95% and 99% C.L. contours in the $\Delta m^2_{21}, B_0$ plane and obtain the corresponding predictions for the Borexino experiment [19]. We also consider fits to the rates separately. Our calculation and fitting procedures are described in detail in our previous papers [5,6,21].

Our investigation proceeds along three main lines. In the first of them we take the ''old'' data set, i.e., the existing data prior to the announcement by the SNO Collaboration of their new charged current (CC) (reduced rate and day/night asymmetry) and NC results [18]. For the neutrino deuteron cross section error values we use the result from a comparison between Refs. [22] and [23]. For the gallium rate we used the value (74.7 ± 5.13) SNU [16]. In the second of these cases we include the SNO newly reported error values for the neutrino deuteron cross sections and CC reduced rate [18]. We also use the combined data from all gallium experiments (72.4 ± 4.7) SNU. Thus the main feature of this second analysis type is a reduction of all error bars, which necessarily results in an increase of the χ^2 in each case. In the third case we add the latest SNO results on CC including the day/night asymmetry and NC [18].

The paper is organized as follows. In Sec. II we present our field profiles in the radiative zone and core, and in the convective zone. We consider seven profiles in the radiative zone and core. As for the convective zone we take three profiles previously investigated in Ref. [5] and one in Ref. [21]. We perform fits to the rates only and global fits in each of the three cases, selecting for the global fits in the radiation zone and core those two that provide the best rate fits. We then select these two from the radiative zone and core and the best two from the convective zone which are used to determine the 95% and 99% C.L. contours around the best fit points. In Sec. III we use these four contours to evaluate the corresponding Borexino predictions. Owing to the characteristic shape of the RSFP survival probability, with a global minimum in the intermediate energy neutrino sector [5], and since Borexino is especially aimed at these neutrinos, the distinction between RSFP and oscillation scenarios will be quite possible with Borexino [20]. For two of the convective zone profiles such predictions were already obtained in Ref. [20] with the ''old'' data set. The comparison between the Borexino predictions obtained with the ''old'' and ''new'' data sets presented here shows that, while the central values remain practically unchanged, the ranges become substantially smaller, owing to the substantial decrease in the error bars. Consequently the possible distinction between the two scenarios (RSFP and oscillations) in Borexino will become even clearer with the present data than before [20]. In Sec. IV we draw our main conclusions. We use throughout the BP'00 value for the ^8B flux [24].

II. RSFP SOLUTIONS

A. Solar field profiles

We present in this subsection the solar field profiles used to obtain the rate and global fits. We start with the core and radiation zone ones (see also Fig. 1).

Profile RZ1:

$$B = B_0 \left[1 - \left(\frac{x - x_c}{x_c} \right)^2 \right], \quad |x| \leqslant x_c, \quad x_c = 0.16, \qquad (1)$$

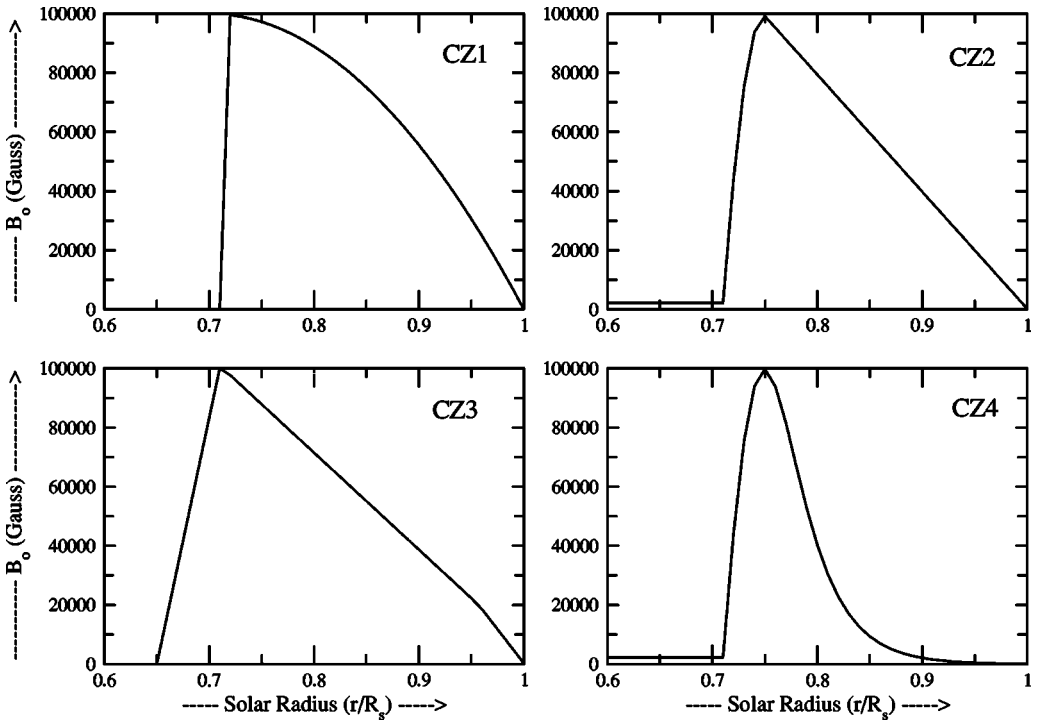

FIG. 2. Solar field profiles in the convective zone. These are selected from previous papers [5,21], where they were found to lead to the best fits in the light of the existing data at the time.

$$B=\frac{B_0}{\cosh[8(x-x_c)]}, \quad x_c\leqslant|x|\leqslant x_m. \tag{2}$$

Profile RZ2:

$$B=B_0\exp\left(-\frac{x}{0.18}\right), \quad |x|\leqslant x_m. \tag{3}$$

Profile RZ3:

$$B=B_0\left[1-\left(\frac{x}{x_m}\right)^2\right], \quad |x|\leqslant x_m. \tag{4}$$

Profile RZ4:

$$B=B_0\left(\frac{x}{x_c}\right), \quad |x|\leqslant x_c, \quad x_c=0.356, \tag{5}$$

$$B=B_0\left[1-\frac{x-x_c}{x_m-x_c}\right], \quad x_c\leqslant|x|\leqslant x_m. \tag{6}$$

Profile RZ5:

$$B=B_0, \quad |x|\leqslant x_c, \quad x_c=0.188, \tag{7}$$

$$B=B_0\exp(-x), \quad x_c\leqslant|x|\leqslant x_m. \tag{8}$$

Profile RZ6:

$$B=\frac{B_0}{\cosh(6x)}|x|\leqslant x_m. \tag{9}$$

Profile RZ7:

$$B=B_0\left(1-\frac{x}{x_m}\right), \quad |x|\leqslant x_m. \tag{10}$$

In all cases x is the fraction of the solar radius ($x=r/R_S$) and $x_m=0.713$, the bottom of the convective zone. All RZ profiles, defined for $x\geqslant 0$, are taken to vanish for $|x|\geqslant x_m$. For the convective zone, we take the following profiles (see also Fig. 2):

Profile CZ1:

$$B=0, \quad x\leqslant x_R, \quad x_R=0.71, \tag{11}$$

$$B=B_0\left[1-\left(\frac{x-0.7}{0.3}\right)^2\right], \quad x\geqslant x_R. \tag{12}$$

Profile CZ2:

$$B=2.16\times 10^3, \quad x\leqslant 0.7105, \tag{13}$$

$$B=B_1\left[1-\left(\frac{x-0.75}{0.04}\right)^2\right], \quad 0.7105<x<0.7483, \tag{14}$$

$$B=1.1494B_0[1-3.4412(x-0.71)], \quad 0.7483\leqslant x\leqslant 1. \tag{15}$$

Profile CZ3:

$$B=0, \quad x\leqslant x_R, \quad x_R=0.65, \tag{16}$$

$$B=B_0\frac{x-x_R}{x_C-x_R}, \quad x_R\leqslant x\leqslant x_C, \quad x_C=0.713, \tag{17}$$

TABLE I. Data from the solar neutrino experiments. Units are SNU for Homestake and gallium and 10^6 cm^{-2} s^{-1} for SuperKamiokande and SNO. See the main text for details.

Experiment	Data	Theory	Data/Theory
Homestake	$2.56\pm0.16\pm0.15$	$7.7\pm^{1.3}_{1.1}$	0.332 ± 0.05
Ga	74.7 ± 5.13	$129\pm^{8}_{6}$	0.58 ± 0.08
Ga (combined)	72.4 ± 4.7	$129\pm^{8}_{6}$	0.56 ± 0.07
SuperKamiokande	2.32 ± 0.085	$5.05\pm^{1.0}_{0.7}$	$0.459\pm0.005\pm^{0.016}_{0.018}$
SNO CC (June 2001)	$1.75\pm0.07\pm^{0.12}_{0.11}\pm0.05$	$5.05\pm^{1.0}_{0.7}$	0.347 ± 0.029
SNO CC (April 2002)	$1.76\pm0.05\pm0.09$	$5.05\pm^{1.0}_{0.7}$	0.349 ± 0.020
SNO CC ($A^{CC}_{D/N}$, April 2002)	$0.14\pm0.063\pm^{0.015}_{0.014}$	0	0
SNO NC	$5.09\pm0.44\pm0.45$	$5.05\pm^{1.0}_{0.7}$	1.01 ± 0.13

$$B=B_0+(x-x_C)\frac{2\times10^4-B_0}{0.957-x_C},\quad x_C\leqslant x\leqslant 0.957, \tag{18}$$

$$B=2.10^4+(x-0.957)\frac{300-2\times10^4}{1-0.957},\quad 0.957\leqslant x\leqslant 1. \tag{19}$$

Profile CZ4:

$$B=2.16\times10^3,\quad x\leqslant 0.7105, \tag{20}$$

$$B=B_1\left[1-\left(\frac{x-0.75}{0.04}\right)^2\right],\quad 0.7105<x<0.7483, \tag{21}$$

$$B=\frac{B_0}{\cosh 30(x-0.7483)},\quad 0.7483\leqslant x\leqslant 1,\quad B_0=0.998B_1. \tag{22}$$

Profiles CZ1, CZ2, and CZ4 are, respectively, profiles 4, 7, and 6 of Ref. [5] and profile CZ3 is profile 4 of Ref. [21]. Also profiles CZ3 and CZ4 were investigated in Ref. [20] as III and II and their Borexino predictions were then derived on the basis of the pre-SNO NC data.

B. Rate fits

The data on rates are summarized in Table I and the RSFP best rate fits for all 11 profiles are presented in Tables II and III. All fits including global ones (Sec. II C) were obtained for the three analysis viewpoints mentioned in the Introduction. Thus we consider the following separately.

(a) Four rates: Chlorine, SuperKamiokande, Ga, and SNO CC total reduced rates. The CC total reduced rate from SNO and its error were taken from their first data announced in June 2001 while the errors for the neutrino deuteron cross sections were taken from a comparison between Kubodera's tables [22] and the Paris potential results [23].

(b) Four rates: Chlorine, SuperKamiokande, Ga (combined), and SNO CC (new) total reduced rates. The CC total rate from SNO and its error as well as the deuteron cross section errors were taken from their data announced in April 2002. These are all substantially smaller than in case (a), resulting in an increase of the χ^2 at the minima and, consequently, in a smaller spread for the Borexino prediction (see Sec. III), owing to the increased steepness of the χ^2.

(c) Six rates: Chlorine, SuperKamiokande, Ga (combined), SNO CC (new) total reduced rates, SNO CC day/night asymmetry ($A^{CC}_{D/N}$), and NC total reduced rate. All errors are as in case (b).

In all cases (a),(b),(c) the free parameters in the analysis are the mass square difference between neutrino flavors Δm^2_{21} and the peak field value B_0. The typical ranges to be investigated are 10^{-7} eV$^2\leqslant\Delta m^2_{21}\leqslant 5\times10^{-6}$ eV^2, 0.1×10^6 G$\leqslant B_0\leqslant 2\times10^6$ G for RZ profiles and 0.7×10^{-8} eV$^2\leqslant\Delta m^2_{21}\leqslant 3\times10^{-8}$ eV^2, 0.1×10^5 G$\leqslant B_0\leqslant 1.5\times10^5$ G for CZ ones. With these choices the number of

TABLE II. Rate fits for solar magnetic field profiles in the radiative zone [Eqs. (1)–(10)]. For each profile the values of Δm^2_{21} and B_0 are given at the best fit together with the corresponding χ^2 and goodness of fit (GOF) for analysis cases (a), (b), and (c), respectively, described in the main text. The values of χ^2_{min} correspond to 2 DOF [cases (a),(b)] and 4 DOF [case (c)]. See the text for more details.

Profile		Δm^2_{21} (eV^2)	$B_0(G)$	χ^2_{rates}	GOF
RZ1	(a)	2.87×10^{-6}	6.79×10^5	3.56	16.9
	(b)	2.86×10^{-6}	7.05×10^5	5.85	5.4
	(c)	2.86×10^{-6}	6.86×10^5	10.7	3.1
RZ2	(a)	2.61×10^{-6}	17.2×10^5	1.47	48.0
	(b)	2.55×10^{-6}	17.4×10^5	1.65	43.8
	(c)	2.57×10^{-6}	17.2×10^5	6.44	16.9
RZ3	(a)	6.85×10^{-6}	2.8×10^5	8.09	1.7
	(b)	6.85×10^{-6}	2.73×10^5	11.1	0.4
	(c)	6.85×10^{-6}	2.95×10^5	14.3	0.63
RZ4	(a)	5.49×10^{-7}	2.21×10^5	9.81	0.6
	(b)	5.54×10^{-7}	2.27×10^5	12.4	0.2
	(c)	5.49×10^{-7}	2.18×10^5	18.7	0.1
RZ5	(a)	4.35×10^{-6}	2.61×10^5	1.61	44.7
	(b)	4.43×10^{-6}	2.57×10^5	3.00	22.3
	(c)	4.04×10^{-6}	2.56×10^5	8.65	7.0
RZ6	(a)	2.64×10^{-6}	10.5×10^5	1.64	44.1
	(b)	2.60×10^{-6}	10.7×10^5	1.97	37.3
	(c)	2.64×10^{-6}	10.4×10^5	6.81	14.6
RZ7	(a)	7.36×10^{-7}	4.01×10^5	7.29	2.6
	(b)	7.23×10^{-7}	4.09×10^5	7.68	2.2
	(c)	7.78×10^{-7}	3.92×10^5	13.7	0.9

TABLE III. Same as Table II for the solar magnetic field profiles in the convective zone [Eqs. (11)–(22)]. The number of DOF is 2 [cases (a),(b)] and 4 [case (c)].

Profile		Δm^2_{21} (eV^2)	$B_0(G)$	χ^2_{rates}	GOF
CZ1	(a)	1.27×10^{-8}	9.7×10^4	0.95	62.2
	(b)	1.15×10^{-8}	9.7×10^4	1.17	55.7
	(c)	1.16×10^{-8}	9.68×10^4	5.87	20.9
CZ2	(a)	1.18×10^{-8}	12.6×10^4	1.17	55.7
	(b)	1.09×10^{-8}	12.6×10^4	1.38	50.0
	(c)	1.09×10^{-8}	12.6×10^4	6.05	19.5
CZ3	(a)	1.42×10^{-8}	9.8×10^4	1.34	51.2
	(b)	1.36×10^{-8}	10.0×10^4	2.14	34.3
	(c)	1.37×10^{-8}	9.92×10^4	6.80	14.7
CZ4	(a)	1.45×10^{-8}	10.9×10^4	1.72	42.3
	(b)	1.43×10^{-8}	11.2×10^4	2.61	27.1
	(c)	1.43×10^{-8}	11.2×10^4	7.39	11.7

degrees of freedom (DOF) is 2 in cases (a) and (b) and 4 in case (c). For profiles RZ1–RZ7, in which case the magnetic field extends over the neutrino production zone, we take for the survival probability the well known formula

$$P=\frac{1}{2}+\left(\frac{1}{2}-P_C\right)\cos 2\theta_i \cos 2\theta_0 \tag{23}$$

with the jump probability P_C given by the Landau-Zener approximation

$$P_C=\exp\left(-\pi\frac{2\mu^2B^2}{\Delta m^2_{21}/2E}0.09R_S\right) \tag{24}$$

and which we integrate over the production regions and energy ranges for each solar neutrino flux. In using this procedure, which avoids the numerical integration of the neutrino evolution equations for each production bin, care must be taken to account for those situations in which neutrinos are produced after the resonance, or the solar density is not large enough to ensure the existence of a resonance, and finally to account for the neutrinos that are produced in the far side of the Sun. The production region and energy spectra were taken from [25].

For the convective zone profiles CZ1–CZ4 the survival probabilities were obtained through the integration of the evolution equations as described in our previous work [5].

The results of the ''rates only'' analysis are shown in Tables II for the radiative zone and III for the convective zone profiles. Generically, it is seen that the quality of the fits depends crucially on which data set is used. From cases (a) to (c) the χ^2 of the fits increases because the uncertainties improve in case (b) relative to (a) and because in case (c) the 2.1σ day/night asymmetry of the CC event rate is taken into account. This confronts the RSFP prediction of zero asymmetry. A comparison between RZ and CZ profiles shows that the ''best'' RZ profiles produce fits of the same approximate quality as the CZ profiles. The latter were chosen to be the ''best'' from our previous experience [5,21]. Hence it is seen that the data clearly show no preference for a magnetic field in either the radiative or the convective zone. It is also noteworthy that RZ profiles (Table II) with the strongest field at the center of the Sun and a rapid decrease away from the center are clearly favored (RZ2,RZ6). The next best is RZ5 which clearly exhibits the same feature. We will select the best two (RZ2,RZ6) to perform the global fits described in the next subsection.

TABLE IV. Global fits for solar magnetic field profiles in the radiative zone [Eqs. (1)–(10)]. The number of DOF is 39 [cases (a),(b)] and 41 [case (c)].

Profile		Δm^2_{21} (eV^2)	$B_0(G)$	χ^2_{global}	GOF
RZ2	(a)	2.61×10^{-6}	16.3×10^5	35.0	65.1
	(b)	2.54×10^{-6}	16.3×10^5	35.0	65.1
	(c)	2.54×10^{-6}	16.7×10^5	40.0	51.4
RZ6	(a)	2.66×10^{-6}	9.97×10^5	35.0	65.5
	(b)	2.59×10^{-6}	9.99×10^5	35.0	65.4
	(c)	2.54×10^{-6}	10.2×10^5	40.1	51.2

C. Global fits

We selected from all seven profiles in the radiative zone (RZ1–RZ7) those two which provide the best rate fits and obtained the corresponding global fits. These are RZ2 and RZ6 (see Tables IV and V). Global fits were performed for all four convective zone profiles. The global fit analysis follows viewpoints (a), (b), and (c) described in Sec. II B with the addition of the SuperKamiokande day/night spectrum for 1258 days [13] (19 day+19 night energy bins) and the exclusion of the total SuperKamiokande rate. This exclusion avoids redundant information already present in the spectral bins and is common to most recent analyses. With these choices the number of DOF is now, in each case, (a),(b) 3 rates+38 spectral bins−2 parameters=39 DOF and (c) 5 rates+38 spectral bins−2 parameters =41 DOF.

TABLE V. Global fits for solar magnetic field profiles in the convective zone [Eqs. (11)–(22)]. The number of DOF is 39 [cases (a),(b)] and 41 [case (c)].

Profile		Δm^2_{21} (eV^2)	$B_0(G)$	χ^2_{global}	GOF
CZ1	(a)	1.25×10^{-8}	9.54×10^4	35.7	61.9
	(b)	1.14×10^{-8}	9.54×10^4	35.7	62.1
	(c)	1.11×10^{-8}	9.60×10^4	40.7	48.4
CZ2	(a)	1.31×10^{-8}	11.0×10^4	36.1	60.1
	(b)	1.22×10^{-8}	11.0×10^4	36.1	60.4
	(c)	1.21×10^{-8}	11.1×10^4	41.1	46.6
CZ3	(a)	1.25×10^{-8}	9.54×10^4	35.7	62.0
	(b)	1.39×10^{-8}	9.67×10^4	35.4	63.6
	(c)	1.38×10^{-8}	9.80×10^4	40.3	50.0
CZ4	(a)	1.38×10^{-8}	10.4×10^4	35.5	63.1
	(b)	1.38×10^{-8}	10.5×10^4	35.6	62.7
	(c)	1.40×10^{-8}	10.8×10^4	40.7	48.4

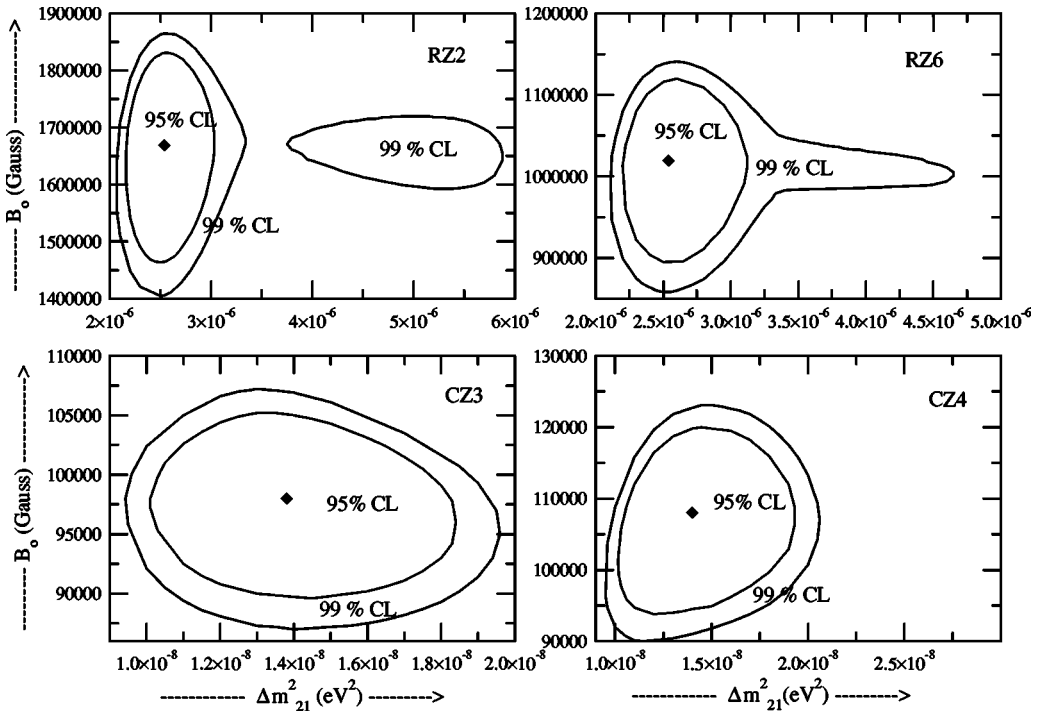

FIG. 3. The 95% and 99% C.L. contours (for 2 DOF $\Delta\chi^2=5.99$ and 9.21, respectively) around the best global fits with analysis procedure (c) for profiles RZ2,RZ6 in the radiative zone and core and CZ3,CZ4 in the convective zone of the Sun. The best fit points are also shown. These correspond to $\chi^2=40.0$ (profile RZ2), $\chi^2=40.1$ (profile RZ6), $\chi^2=40.3$ (profile CZ3), $\chi^2=40.7$ (profile CZ4) with 41 DOF. See also Tables IV and V.

The global fits obtained for the selected profiles in the radiative zone and core are shown in Table IV and those for the convective zone in Table V. It is seen that the quality of the global fits is the same for the best two profiles in the radiative zone (RZ2,RZ6) on one hand and all chosen four convective zone ones on the other (these were chosen as the best from our previous experience). All six exhibit a χ^2_{global} roughly equal to or slightly smaller than the number of DOF. As in the case of the analysis of rates only, the radiative zone profiles that seem favored by the data are those for which the field is the strongest at the solar center with an almost immediate rapid decrease away from the center. Hence the favored magnetic field profiles appear to satisfy a dipole structure centered in the solar center. Their shape also much resembles the solar matter density shape.

For the best profile in the radiative zone (RZ2) and the best one in the convective zone (CZ3) we show in the following the predictions at the best global fits for the experimentally measured quantities in cases (c) (all new data). These are global fits 2(c) in Table IV and 3(c) in Table V which the reader can compare with the data given in Table I:

Profile RZ2, $\chi^2_{gl}=40.01$(41 DOF);
$R_{\rm Ga}=72.5$ SNU, $R_{\rm Cl}=2.64$ SNU, $R_{SNO,CC}=0.354$;
$A^{CC}_{D/N}=0$, $R_{SNO,NC}/R^{st}_{SNO,CC}=0.968$;
Profile CZ3, $\chi^2_{gl}=40.34$ (41 DOF);
$R_{\rm Ga}=72.5$ SNU, $R_{\rm Cl}=2.45$ SNU, $R_{SNO,CC}=0.364$;
$A^{CC}_{D/N}=0$, $R_{SNO,NC}/R^{st}_{SNO,CC}=0.968$.

All predictions are well within 1σ of the measured data, except for the $A^{CC}_{D/N}$ asymmetry whose RSFP prediction is strictly zero.

Finally we choose the two radiative zone and the two convective zone profiles providing the best global fits in case (c) to evaluate the 95% C.L. (1.96σ) and 99% C.L. (2.58σ) allowed regions in the $\Delta m^2_{21}, B_0$ plane. These global fits are 2(c),6(c) in Table IV and 3(c),4(c) in Table V and the contours of the allowed regions are shown in Fig. 3. They are defined as the set of points satisfying $\chi^2(\Delta m^2_{21}, B_0)-\chi^2_{min}=\Delta\chi^2$(C.L.,2 DOF) with $\Delta\chi^2$(C.L.,2 DOF)$=5.99$ and 9.21 for 95% C.L. and 99% C.L., respectively. They will be used to evaluate the predictions for the Borexino experiment in the next section.

III. PREDICTIONS FOR BOREXINO EXPERIMENT

Except for the possible direct evidence that Kamland [9] may provide of the LMA solution, thus excluding RSFP as the dominant process for the solar neutrino deficit, no experiment other than Borexino is able to provide a positive distinction between oscillation solutions and RSFP. Hence it is essential to investigate the ''best'' RSFP predictions for Borexino. We chose the ''best'' two profiles in the radiative zone (RZ2,RZ6) and in the convective zone (CZ3,CZ4) and evaluated Borexino predictions at their best global fits, 2(c),6(c) (Table IV) and 3(c),4(c) (Table V). We also give in each case the upper and lower 95% and 99% C.L.'s around the central values. These predictions, given as ratios between RSFP event rates and standard event rates, and their confidence ranges are shown in Table VI. The analysis procedure, case (c) described in Sec. II C, involves all currently available solar neutrino data and best estimates for the errors.

TABLE VI. Predicted reduced event rates (rates assuming RSFP divided by the standard solar model predictions) for Borexino using all ''new'' data [case (c)].

Profile	Best fit	min (95% C.L.)	max (95% C.L.)	min (99% C.L.)	max (99% C.L.)
RZ2	0.46	0.40	0.54	0.40	0.56
RZ6	0.44	0.38	0.52	0.37	0.54
CZ3	0.34	0.32	0.45	0.30	0.50
CZ4	0.39	0.30	0.54	0.29	0.57

Borexino predictions from RSFP were evaluated earlier [20] for profiles CZ3,CZ4 (profiles III,II, respectively, in Ref. [20]) with the available data as of December 2001. They were $0.35^{+0.22}_{-0.05}$ and $0.41^{+0.21}_{-0.13}$, respectively, for the 99% C.L. Comparing these with Table VI it is seen that, while the central values hardly change, exhibiting a slight tendency for a decrease ($\simeq 4\%$), the smaller errors from the neutrino deuteron cross sections and from the SNO and Ga rates lead to a sizable reduction of the C.L. intervals. Such a reduction is also observed in the oscillation predictions [26]. For RSFP this is mainly reflected in a decrease of the 95% and 99% C.L. upper limits, leading to the possibility of an even clearer distinction between RSFP and oscillation signatures in the Borexino experiment with the new data. In fact for the LMA solution such a distinction is possible to more than 5.7σ for all four profiles examined, whereas for the low probability, low mass (LOW) solution all predictions are more than 4.5σ away (see Table 2 of Ref. [26] and our Table VI). The only possible model dependence of RSFP predictions is contained in the choice of the magnetic field profile, but this choice is severely constrained by the requirement of fitting all solar data.

IV. SUMMARY AND CONCLUSIONS

Our main conclusions can be summarized in Tables IV and V [cases labeled (c)], Fig. 3, and Table VI.

The objective of this paper is to present a statistical analysis of all available solar neutrino data in the light of the RSFP solution to the solar neutrino problem, after the recent presentation of the SNO neutral current results. In addition to global fits and since these give, through the large number of spectral bins involved, a great significance to one single experiment, we also performed a separate analysis of rates only. Since the localization of the strongest solar field is still unclear, we considered solar magnetic field profiles both in the radiative zone and core, and in the convective zone of the Sun.

The RSFP solutions do not predict any day/night effect, nor do they imply any dependence of observable solar neutrino flux which follows the sunspot activity. Also on the basis of the chlorine, SuperKamiokande, and SNO experiments it will be very hard to exclude RSFP solutions if the day/night asymmetries in SuperKamiokande and SNO remain consistent with zero. This difficulty is related to the fact that in the relevant solar neutrino energy ranges for these experiments, the survival probability shape looks much the same for both RSFP [5] and the preferred oscillation solutions, LMA and LOW [26]. On the other hand, gallium experiments will also be unable to tell the difference, in particular if only time averaged data are considered [27]. Such a ''negative'' situation is, however, counterbalanced by the major difference in the above mentioned survival probability shapes in the intermediate energy neutrino sector, mainly Be, at which the Borexino experiment is directly aimed. Hence the importance of Borexino predictions which we also investigated. Such predictions were performed previously [20] and they showed a clear distinction between the two scenarios which, on the basis of the new data, has become better.[2]

Altogether, radiative zone and core field profiles on one hand and convective zone ones on the other are equally favored by the data with fits of the same quality as the best oscillation solution, the LMA one [26]. For profiles in the radiative zone and core the data clearly prefer a strong field at the center of the Sun with a rapid decrease thereafter. Interestingly enough this shape of profiles follows a dipole structure centered at the solar center and closely resembles the density profile of the Sun.

Specific time signatures of the RSFP mechanism may be related to the possible nonaxially symmetric character of the solar field or the inclination of the Earth's orbit. In the first case a time dependence would appear as a variation of the event rate with a period of 28 days, while in the second the possible polar angle dependence of the solar field would cause a seasonal variation of the rate. Averaging rates over time erases all time dependent information that may be contained in the data. In fact a statistical analysis on the gallium data performed by the Stanford group [27] shows the existence of two peaks in the event rates, which, while not providing conclusive evidence for RSFP, cannot be explained on the grounds of oscillations. It will be very important to independently repeat such analyses and to analyze the data in time bins in the future, especially if Kamland shows a negative result.

ACKNOWLEDGMENTS

We acknowledge useful discussions with Evgeni Akhmedov and André de Gouvêa and correspondence with C. Peña-Garay. B.C.C. was supported by Fundação para a Ciência e Tecnologia through award ref. SFRH/BPD/5719/2001.

[2]There is a caveat here, however, due to the intrinsic error of the Borexino experiment [28].

[1] A. Cisneros, Astrophys. Space Sci. **10**, 87 (1971).
[2] C. S. Lim and W. J. Marciano, Phys. Rev. D **37**, 1368 (1988); E. Kh. Akhmedov, Yad. Fiz. **48**, 599 (1988) [Sov. J. Nucl. Phys. **48**, 382 (1988)]; Phys. Lett. B **213**, 64 (1988).
[3] L. Wolfenstein, Phys. Rev. D **17**, 2369 (1978); S. P. Mikheyev and A. Yu. Smirnov, Yad. Fiz. **42**, 1441 (1985) [Sov. J. Nucl. Phys. **42**, 913 (1985)].
[4] M. M. Guzzo and H. Nunokawa, Astropart. Phys. **12**, 87 (1999).
[5] J. Pulido and E. K. Akhmedov, Astropart. Phys. **13**, 227 (2000).
[6] E. K. Akhmedov and J. Pulido, Phys. Lett. B **485**, 178 (2000).
[7] O. G. Miranda, C. Peña-Garay, T. I. Rashba, V. B. Semikoz, and J. W. Valle, Nucl. Phys. **B595**, 360 (2001).
[8] A. M. Gago, M. M. Guzzo, P. C. de Holanda, H. Nunokawa, O. L. Peres, V. Pleitez, and R. Zukanovich Funchal, Phys. Rev. D **65**, 073012 (2002).
[9] P. Alivisatos *et al.*, Report No. STANFORD-HEP-98-03; Kamland Collaboration, A. Piepke, Nucl. Phys. B (Proc. Suppl.) **91**, 99 (2001).
[10] J. Pulido, Phys. Rev. D **57**, 7108 (1998).
[11] See, e.g., E. N. Parker, in *Proceedings of the VI Canary Islands School*, edited by Roca Cortes and F. Sanchez (Cambridge University Press, Cambridge, England, 1996), p. 229; H. M. Antia, S. M. Chitre, and M. J. Thompson, Astron. Astrophys. **360**, 335 (2000).
[12] A. Friedland and A. Gruzinov, hep-ph/0202095.
[13] SuperKamiokande Collaboration, S. Fukuda *et al.*, Phys. Rev. Lett. **86**, 5651 (2001).
[14] Homestake Collaboration, B. T. Cleveland *et al.*, Astrophys. J. **496**, 505 (1998).
[15] SAGE Collaboration, J. N. Abdurashitov *et al.*, Phys. Rev. C **60**, 055801 (1999); SAGE Collaboration, J. N. Abdurashitov *et al.*, Yad. Fiz. **63**, 1019 (2000) [Phys. At. Nucl. **63**, 943 (2000)]; SAGE Collaboration, J. N. Abdurashitov *et al.*, astro-ph/0204245.
[16] GALLEX Collaboration, W. Hampel *et al.*, Phys. Lett. B **447**, 127 (1999); M. Altmann *et al.*, *ibid.* **490**, 16 (2000); E. Bellotti, Nucl. Phys. B (Proc. Suppl.) **91**, 44 (2001).
[17] SNO Collaboration, Q. R. Ahmad *et al.*, Phys. Rev. Lett. **87**, 071301 (2002).
[18] SNO Collaboration, Q. R. Ahmad *et al.*, Phys. Rev. Lett. **89**, 011301 (2002); **89**, 011302 (2002).
[19] Borexino Collaboration, G. Alimonti *et al.*, Astropart. Phys. **16**, 205 (2002).
[20] E. K. Akhmedov and J. Pulido, Phys. Lett. B **529**, 193 (2002).
[21] J. Pulido, hep-ph/0112104.
[22] K. Kubodera homepage, http://nuc003.psc.sc.edu/ kubodera/
[23] S. Ying, W. C. Haxton, and E. M. Henley, Phys. Rev. C **45**, 1982 (1992).
[24] J. N. Bahcall, M. H. Pinsonneault, and S. Basu, Astrophys. J. **555**, 990 (2001).
[25] J. N. Bahcall homepage, http://www.sns.ias.edu/ jnb/
[26] J. N. Bahcall, M. C. Gonzalez-Garcia, and C. Peña-Garay, hep-ph/0204314.
[27] P. A. Sturrock and J. D. Scargle, Astrophys. J. Lett. **550**, L101 (2001).
[28] A. de Gouvêa, A. Friedland, and H. Murayama, Phys. Rev. D **60**, 093011 (1999).